

NIKHEF 04-007

July 2004

THE THREE-LOOP SPLITTING FUNCTIONS IN QCD

A. VOGT*, S. MOCH[†], J.A.M. VERMASEREN*

*NIKHEF, Kruislaan 409, 1098 SJ Amsterdam, The Netherlands
 E-mails: avogt@nikhef.nl and t68@nikhef.nl

[†]DESY-Zeuthen, Platanenallee 6, D-15735 Zeuthen, Germany
 E-mail: moch@ifh.de

We have computed the next-to-next-to-leading-order (NNLO) contributions to the evolution of unpolarized parton distributions in perturbative QCD [1,2]. In this talk, we briefly recall why this huge computation was necessary and outline how it was performed. We then illustrate the structure of the results and discuss their end-point limits which include the three-loop cusp anomalous dimensions of the Wilson lines. Finally the numerical impact of the new contributions is illustrated.

1 Introduction

For the next decade, the highest-energy experiments in particle physics will be done at the (anti-)proton–proton colliders TEVATRON and LHC. At such machines, if we disregard power corrections and observables involving final-state fragmentation functions, the cross sections for hard processes h can be schematically written as

$$\sigma_h^{pp} = \sum_{f,f'} f_p * f'_p * \hat{\sigma}_h^{ff'} . \quad (1.1)$$

Here f_p stands for the universal momentum distributions of the partons f in the proton, $f = q_i, \bar{q}_i, g$ with $i = 1, \dots, n_f$, where n_f is the number of effectively massless quark flavours. $\hat{\sigma}_h^{ff'}$ represent the hard (partonic) cross sections for the process under consideration. Hence quantitative studies of the standard model, and of expected and unexpected new particles, require a precise understanding of the partonic luminosities and of the QCD corrections to the corresponding cross sections.

For many important processes, like Higgs-boson production, the second-order (NNLO) QCD corrections need to be taken into account, i.e., the third term in

$$\hat{\sigma}_h = a_s^{n_h} \left[\hat{\sigma}_h^{(0)} + a_s \hat{\sigma}_h^{(1)} + a_s^2 \hat{\sigma}_h^{(2)} + \dots \right] . \quad (1.2)$$

The consistent inclusion of $\hat{\sigma}_h^{(2)}$ in Eq. (1.1) requires parton distributions evolved with the corresponding (process-independent) NNLO splitting functions

$$P_{ff'}^{\text{NNLO}} = a_s P_{ff'}^{(0)} + a_s^2 P_{ff'}^{(1)} + a_s^3 P_{ff'}^{(2)} . \quad (1.3)$$

The one- and two-loop splitting functions have been known for a long time [3]–[11]. For the three-loop splitting functions $P^{(2)}$, on the other hand, only partial results had been obtained until recently [12]–[22]. However earlier this year we have, finally, computed the complete expressions of these functions [1,2].

2 Outline of the calculation

We have derived the NNLO splitting functions by computing the partonic structure functions in inclusive deep-inelastic scattering (DIS), $\gamma^*(q) + f(p) \rightarrow X$ with $Q^2 \equiv -q^2 > 0$ and $p^2 = 0$, up to the third order in the strong coupling $a_s = \alpha_s/(4\pi)$. This computation has been performed for all even or odd values of the Mellin variable N via the three-loop forward Compton amplitudes, $\gamma^*(q) + f(p) \rightarrow \gamma^*(q) + f(p)$.

This approach has two major advantages: Firstly it enables us to obtain, at almost the same time, also the three-loop coefficient functions in DIS [23]. Secondly it allows us to check our programs, at almost any stage, by falling back to the MINCER program [24,25] employed in the fixed- N calculations of refs. [12]–[14].

2.1 Mass-factorization in DIS

Before we address the main computational task, we briefly sketch how the splitting functions are extracted from the calculation. We start by writing the physical structure functions F_a in terms of the (perturbatively calculable) bare partonic structure functions $\tilde{F}_{a,k}$, the bare coupling \tilde{a}_s and the bare parton distributions \tilde{f}_k ,

$$F_a(Q^2) = \tilde{F}_{a,k}(\tilde{a}_s, Q^2, \varepsilon) * \tilde{f}_k . \quad (2.1)$$

Summation over the parton species k is understood, and $*$ stands for either the convolution in Bjorken- x space or a simple multiplication of the Mellin moments. As indicated in Eq. (2.1), we use dimensional regularization with $D = 4 - 2\varepsilon$, thus the singularities of $\tilde{F}_{a,k}$ appear as poles ε^{-l} . After the ultraviolet divergences have been removed by coupling-constant renormalization, at the renormalization scale μ_r , only initial-state mass singularities remain. They arise when two momenta become collinear, e.g., p and k in Fig. 1, leading to propagator denominators

$$(p - k)^2 = -2|\vec{p}||\vec{k}|(1 - \cos \vartheta) \xrightarrow{\vartheta \rightarrow 0} -|\vec{p}||\vec{k}|\vartheta^2 .$$

These singularities are removed by mass factorization, at the factorization scale μ_f : $\tilde{F}_{a,k}$ is decomposed into finite pieces, the coefficient functions $C_{a,i}$, and the universal transition functions Γ_{ik} which contain the (a -independent) pole parts of $\tilde{F}_{a,k}$. The latter are combined with the \tilde{f}_k to form the finite renormalized parton densities f_i ,

$$\begin{aligned} F_a(Q^2) &= \tilde{F}_{a,k}(a_s(\mu_r^2), \frac{Q^2}{\mu_r^2}, \varepsilon) * \tilde{f}_k \underbrace{f_i(\mu_f^2, \mu_r^2)}_{= C_{a,i}(a_s(\mu_r^2), \frac{Q^2}{\mu_f^2}, \frac{\mu_f^2}{\mu_r^2}, \varepsilon) * \Gamma_{ik}(a_s(\mu_r^2), \frac{\mu_f^2}{\mu_r^2}, \varepsilon) * \tilde{f}_k} . \end{aligned} \quad (2.2)$$

The decomposition (2.2) is not unique. We employ the usual $\overline{\text{MS}}$ scheme where, besides the $1/\varepsilon$ poles, only the artefacts $S_\varepsilon = \exp(\varepsilon[\ln(4\pi) - \gamma_e])$ of dimensional regularization are removed from the coefficient functions. Differentiation of Eq. (2.2) finally leads to the evolution equations for the renormalized parton distributions,

$$\frac{\partial}{\partial \ln \mu_f^2} f_i = \frac{\partial \Gamma_{ik}}{\partial \ln \mu_f^2} * \tilde{f}_k = \frac{\partial \Gamma_{ik}}{\partial \ln \mu_f^2} * \Gamma_{kj}^{-1} * f_j \equiv P_{ij} * f_j . \quad (2.3)$$

The splitting functions (1.3) can thus be obtained from the $1/\varepsilon$ poles in Eq. (2.2).

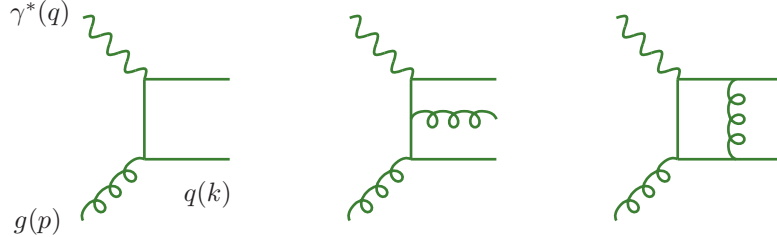


Figure 1. Sample diagrams contributing to the inclusive process $\gamma^* g \rightarrow X$ up to third order in a_s .

2.2 The flavour decomposition

It is convenient to decompose the system (2.3) of $2n_f + 1$ coupled equation as far as possible from charge conjugation and flavour symmetry constraints alone. The general structure of the (anti-)quark (anti-)quark splitting functions reads

$$\begin{aligned} P_{q_i q_k} &= P_{\bar{q}_i \bar{q}_k} = \delta_{ik} P_{qq}^v + P_{qq}^s \\ P_{q_i \bar{q}_k} &= P_{\bar{q}_i q_k} = \delta_{ik} P_{q\bar{q}}^v + P_{q\bar{q}}^s . \end{aligned} \quad (2.4)$$

This structure leads to three independently evolving types of flavour non-singlet combinations. The flavour asymmetries q_{ns}^\pm and the total valence distribution q_{ns}^v ,

$$q_{ns,ik}^\pm = q_i \pm \bar{q}_i - (q_k \pm \bar{q}_k) , \quad q_{ns}^v = \sum_{r=1}^{n_f} (q_r - \bar{q}_r) , \quad (2.5)$$

respectively evolve with

$$\begin{aligned} P_{ns}^\pm &= P_{qq}^v \pm P_{q\bar{q}}^v , \\ P_{ns}^v &= P_{qq}^v - P_{q\bar{q}}^v + n_f (P_{qq}^s - P_{q\bar{q}}^s) \equiv P_{ns}^- + P_{ns}^+ . \end{aligned} \quad (2.6)$$

The singlet quark distribution, $q_s = \sum_{r=1}^{n_f} (q_r + \bar{q}_r)$ is coupled to gluon density g ,

$$\frac{d}{d \ln \mu_f^2} \begin{pmatrix} q_s \\ g \end{pmatrix} = \begin{pmatrix} P_{qq} & P_{qg} \\ P_{gq} & P_{gg} \end{pmatrix} * \begin{pmatrix} q_s \\ g \end{pmatrix} , \quad (2.7)$$

where the quark-quark splitting function P_{qq} can be expressed as

$$P_{qq} = P_{ns}^+ + n_f (P_{qq}^s + P_{q\bar{q}}^s) \equiv P_{ns}^+ + P_{ps} . \quad (2.8)$$

The off-diagonal entries in Eq. (2.7) are given by

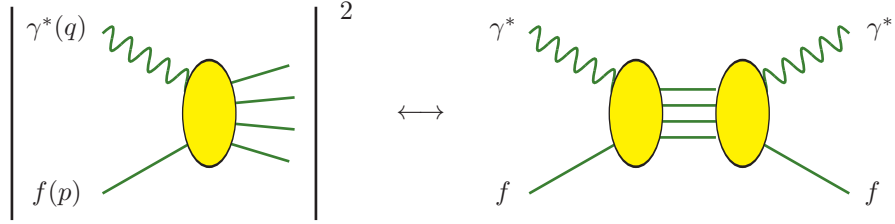
$$P_{qg} = n_f P_{q_i g} , \quad P_{gq} = P_{gq_i} \quad (2.9)$$

in terms of the flavour-independent splitting functions $P_{q_i g} = P_{\bar{q}_i g}$ and $P_{gq_i} = P_{g\bar{q}_i}$.

In the expansion in powers of a_s , the flavour-diagonal ('valence') quantity P_{qq}^v in Eq. (2.4) starts at first order. $P_{q\bar{q}}^v$ and the flavour-independent ('sea') contributions P_{qq}^s and $P_{q\bar{q}}^s$ – and hence the 'pure-singlet' term P_{ps} – are of order α_s^2 . A non-vanishing $P_{ns}^s = P_{qq}^s - P_{q\bar{q}}^s$ in Eq. (2.6) occurs for the first time at the third order and introduces a new colour structure, $d_{abcd} d_{abc}$. See Fig. 1b of ref. [26] for a typical diagram contributing to P_{ns}^s .

2.3 Set-up of the calculation

Diagrams like those in Fig. 1 have been calculated directly, by working out the phase-space integrations, for the derivation of the complete second-order coefficient functions [27]–[30]. An extension of this procedure to the third order, however, does not seem feasible. Instead, we employ the optical theorem



to transform the problem into forward Compton amplitudes. We then make use of a theorem [31] that the coefficient of $(2p \cdot q)^N$ provides the N -th Mellin moment,

$$\tilde{F}(N) = \int_0^1 dx x^{N-1} \tilde{F}(x) ,$$

of the partonic structure functions (2.1) which we need to calculate.

In order to obtain the complete set of the third-order contributions to the splitting functions (2.6) and (2.7) we have to include, besides the photon shown above, also the W -boson [26] – for accessing P_{ns}^- and P_{ns}^s – and a fictitious classical scalar ϕ coupling directly only to the gluon field via $\phi G_{\mu\nu}^a G_a^{\mu\nu}$ [32,33] – for accessing P_{gq} and P_{gg} . Especially the latter leads to a substantial increase of the number of diagrams (generated with QGRAF [34]) as shown in Table 1. Among the partons f we also include the standard ghost h . This allows us to take the sum over external gluon spins by contracting with $-g_{\mu\nu}$ instead of the full physical expression.

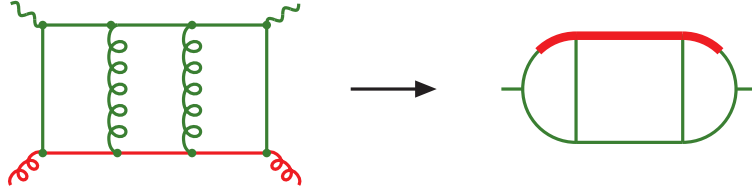
	tree	1-loop	2-loop	3-loop
q γ	1	3	25	359
g γ		2	17	345
h γ			2	56
q W	1	3	32	589
q ϕ		1	23	696
g ϕ	1	8	218	6378
h ϕ		1	33	1184
sum	3	18	350	9607

Table 1. The number of diagrams employed in our calculation of the three-loop splitting functions.

Obviously a highly efficient symbolic treatment is needed to cope with the task at hand. Unsurprisingly, we use FORM for all manipulations. Note that the capabilities of this program had to be extended substantially for this computation [35,36].

2.4 Treatment of the integrals

Finally we illustrate the computation of the integrals required to evaluate the forward Compton amplitudes. One of the 9607 three-loop diagrams in Table 1 is shown here together with a useful pictorial representation of its momentum flow:



For the latter we temporarily disregard the external parton lines and draw the remaining self-energy type diagram, the topology of which is denoted following the notation of ref. [25]. Our example is a ladder (LA) diagram. The (partly additional) denominators carrying the parton momentum p are then indicated by the fat (in the coloured version: red) lines. Here p runs, after turning the diagram upside-down, through the lines 1, 2 and 3, thus the example is assigned the subtopology LA₁₃.

According to our discussion in the previous subsection, we need analytic expressions for the (dimensionless) coefficients $I(N)$ of $(2p \cdot q)^N / Q^{2\alpha}$. One might try to obtain $I(N)$ by brute force, Taylor-expanding the denominators with p and working out the sums. It turns out that such a strategy, in general, does not work. Instead, we employ identities based on integration by parts, scaling arguments and form-factor decompositions (see Sect. 2 of ref. [1]) to successively simplify the integrals.

The LA₁₃ integrals, e.g., can be simplified by applying $p^\mu \partial / \partial q^\mu$ both inside and outside the integral. For the scalar integral with unit denominators this yields

$$\begin{aligned}
 & \text{Diagram with red line and labels 1} = \\
 & -\frac{N+3+3\epsilon}{N+2} \frac{2p \cdot q}{q^2} \text{Diagram with red line and labels 1} + \frac{2}{N+2} \text{Diagram with red line and label 2}
 \end{aligned} \tag{2.10}$$

Here the LA₁₃ integral occurs twice, once with a prefactor $2p \cdot q$. Hence Eq. (2.10) represents a difference equation (here of order $n = 1$) which expresses its coefficient $I(N)$ in terms of that of a LA₁₂ integral with an enhanced denominator in the 3-line,

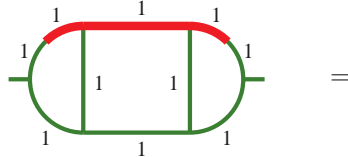
$$a_0(N)I(N) - \dots - a_n(N)I(N-n) - G(N) = 0. \tag{2.11}$$

First-order recursion relations like Eq. (2.10) can be reduced to a sum. Higher-order recursions (we have used equations up to $n = 4$) can be solved by inserting a suitable ansatz into Eq. (2.11). Both procedures make use of the fact that all integrals required for the computation of the splitting functions can be expressed

in terms of harmonic sums [37]. Recall that these sums are recursively defined by

$$S_{\pm m}(M) = \sum_{i=1}^M \frac{(\pm 1)^i}{i^m}, \quad S_{\pm m_1, m_2, \dots, m_k}(M) = \sum_{i=1}^M \frac{(\pm 1)^i}{i^{m_1}} S_{m_2, \dots, m_k}(i). \quad (2.12)$$

To the accuracy in the dimensional offset ε required for the calculation of the splitting functions, our example integral reads, using the FORM notations $\text{den}(i+N)$ for $1/(N+i)$ and $S(R(m_1, \dots, m_k), i+N)$ for $S_{m_1, \dots, m_k}(N+i)$,



$$= \quad (2.13)$$

$$\begin{aligned}
& +\text{theta}(N)*\text{sign}(N)*\text{ep}^{-2}*(-8/3*\text{den}(1+N)^2-4*\text{den}(1+N)^3+8/3*\text{den}(1+N)^2*2*S(R(1), 1+N)+4/3*\text{den}(1+N)*S(R(1), 1+N)+2/3*\text{den}(1+N)*S(R(2), 1+N)-4/3*\text{den}(2+N)^2-2*\text{den}(2+N)^3+4/3*\text{den}(2+N)^2*2*S(R(1), 2+N)+4/3*\text{den}(2+N)*S(R(1), 2+N)+2/3*\text{den}(2+N)*S(R(2), 2+N)+4/3*S(R(1), N)+2/3*S(R(1, 2), N)-2*S(R(2), N)-4/3*S(R(2), N)*N+4*S(R(2, 1), N)+4/3*S(R(2, 1), N)*N-6*S(R(3), N)-2*S(R(3), N)*N) \\
& +\text{theta}(N)*\text{sign}(N)*\text{ep}^{-1}*(32*\text{den}(1+N)^2+164/3*\text{den}(1+N)^3+24*\text{den}(1+N)^4-20/3*\text{den}(1+N)^3*S(R(1), 1+N)-88/3*\text{den}(1+N)^2*2*S(R(1, 1), 1+N)-40/3*\text{den}(1+N)^2*2*S(R(2), 1+N)-16*\text{den}(1+N)*S(R(1), 1+N)+8/3*\text{den}(1+N)*S(R(1, 1), 1+N)+10/3*\text{den}(1+N)*S(R(1, 2), 1+N)-58/3*\text{den}(1+N)*S(R(2), 1+N)+10*\text{den}(1+N)*S(R(2, 1), 1+N)-18*\text{den}(1+N)*S(R(3), 1+N)+16*\text{den}(2+N)^2+82/3*\text{den}(2+N)^3+12*\text{den}(2+N)^4-10/3*\text{den}(2+N)^3*S(R(1), 2+N)-44/3*\text{den}(2+N)^2*2*S(R(1), 2+N)-6*\text{den}(2+N)^2*2*S(R(2), 2+N)-16*\text{den}(2+N)*S(R(1), 2+N)+8/3*\text{den}(2+N)*S(R(1, 1), 2+N)+10/3*\text{den}(2+N)*S(R(1, 2), 2+N)-46/3*\text{den}(2+N)*S(R(2), 2+N)+6*\text{den}(2+N)*S(R(2, 1), 2+N)-12*\text{den}(2+N)*S(R(3), 2+N)-20*S(R(1), N)+8/3*S(R(1, 1), N)+10/3*S(R(1, 1, 2), N)-16*S(R(1, 2), N)-4*S(R(1, 2), N)*N+14*S(R(1, 2, 1), N)+4*S(R(1, 2, 1), N)*N-24*S(R(1, 3), N)-6*S(R(1, 3), N)*N+56/3*S(R(2), N)+20*S(R(2), N)*N-134/3*S(R(2, 1), N)-56/3*S(R(2, 1), N)*N+16/3*S(R(2, 1, 1), N)+8/3*S(R(2, 1, 1), N)*N-62/3*S(R(2, 2), N)-22/3*S(R(2, 2), N)*N+76*S(R(3), N)+100/3*S(R(3), N)*N-10*S(R(3, 1), N)-10/3*S(R(3, 1), N)*N+36*S(R(4), N)+12*S(R(4), N)*N) .
\end{aligned}$$

Despite being uncharacteristically simple in both derivation and size, Eq. (2.10) illustrates the strict hierarchy of subtopologies in our procedure. Our LA_{13} example can only be evaluated once the LA_{12} integral in Eq. (2.10) is known. This integral, in turn, requires the so-called basic building blocks (with only one p -dependent denominator) LA_{11} and LA_{22} together with other integrals of simpler topologies where one of the non- p denominators has been removed. Also those integrals need to be evaluated in terms of yet simpler cases, and so on.

Constructing the reduction chains for all subtopologies, and computing all integrals required for evaluating either diagrams or other, higher-level integrals took literally years of both human and computing resources. It would not have been possible to get through without extensive tabulation of intermediate results for which new features were added to FORM [36]. At the end, a database had been accumulated of more than 100 000 integrals requiring about 3.5 GBytes of disk space.

3 Sample results in N -space and x -space

We illustrate our final results by writing down the even- N anomalous dimensions and the corresponding x -space splitting functions in Quantum-Gluodynamics, i.e., for QCD with $n_f = 0$ quark flavours. The complete QCD results in refs. [1,2] are considerably longer, by a factor of about 15, but not structurally more complicated.

3.1 Expressions in Mellin- N space

We start in N -space where, as discussed above, the actual calculations have been performed. Recall that we expand in terms of $a_s = \alpha_s/(4\pi)$, and that $\gamma^{(n)}(N) = 1 - P^{(n)}(N)$ is the coefficient of a_s^{n+1} . Here we hide N -dependent denominators by using differences of harmonic sums at suitably shifted arguments for which we employ the abbreviations

$$N_{\pm i} S_{\vec{m}} \equiv S_{\vec{m}}(N \pm i) , \quad N_{\pm} \equiv N_{\pm 1} .$$

In this notation the well-known one- and two-loop results [3,4,7,10,11] are given by

$$\gamma_{gg}^{(0)}(N) = C_A \left(4(N_{-2} - 2N_{-} - 2N_{+} + N_{+2} + 3) S_1 - \frac{11}{3} \right) , \quad (3.1)$$

$$\begin{aligned} \gamma_{gg}^{(1)}(N) = & 4 C_A^2 \left(-4(N_{-2} - 2N_{-} - 2N_{+} + N_{+2} + 3) \left[S_{1,-2} + S_{1,2} + S_{2,1} \right] \right. \\ & + \frac{8}{3}(N_{+} - N_{+2}) S_2 - 4(N_{-} - 3N_{+} + N_{+2} + 1) \left[3S_2 - S_3 \right] + \frac{109}{18}(N_{-} + N_{+}) S_1 \\ & \left. + \frac{61}{3}(N_{-} - N_{+}) S_2 - \frac{8}{3} + 2S_{-3} - \frac{14}{3}S_1 + 2S_3 \right) . \end{aligned} \quad (3.2)$$

The three-loop gluon-gluon anomalous dimension [2] reads, for $n_f = 0$,

$$\begin{aligned} \gamma_{gg}^{(2)}(N) = & 16 C_A^3 \left((N_{-2} - 2N_{-} - 2N_{+} + N_{+2} + 3) \left[\frac{73091}{648} S_1 - 16S_{1,-4} + \frac{88}{3}S_{1,-3} \right. \right. \\ & + 16S_{1,-3,1} + \frac{85}{6}S_{1,-2} + 4S_{1,-2,-2} - 11S_{1,-2,1} + 4S_{1,-2,2} - \frac{413}{108}S_{1,1} + 24S_{1,1,-3} \\ & + 11S_{1,1,-2} - 16S_{1,1,-2,1} + 8S_{1,1,3} - \frac{67}{9}S_{1,2} + 8S_{1,2,-2} + 8S_{1,2,2} + \frac{55}{3}S_{1,3} + 8S_{1,3,1} \\ & - 8S_{1,4} - \frac{395}{27}S_2 - 14S_{2,-3} - \frac{11}{3}S_{2,-2} + 8S_{2,-2,1} - \frac{67}{9}S_{2,1} + 4S_{2,1,-2} + 8S_{2,1,2} \\ & + \frac{22}{3}S_{2,2} + 8S_{2,2,1} - 10S_{2,3} + 8S_{3,1,1} - 8S_{3,2} \left. \right] + (2 - N_{-} - N_{+}) \left[\frac{713}{324}S_1 + \frac{26}{3}S_{1,-3} \right. \\ & - 14S_{1,-2,1} + \frac{61}{9}S_{1,-2} + \frac{80}{27}S_{1,1} - 14S_{1,1,-2} + \frac{109}{18}S_{1,2} - 4S_{1,3} \left. \right] + (N_{-} - N_{+}) \left[\frac{473}{216}S_2 \right. \\ & - 12S_{2,-3} + 5S_{2,-2} - 2S_{2,1} - 8S_{2,1,-2} + \frac{23}{3}S_{2,2} - 10S_{2,3} + \frac{665}{36}S_3 - 20S_{3,-2} + \frac{34}{3}S_{3,1} \\ & - 16S_{3,2} - 21S_4 - 26S_{4,1} \left. \right] + (N_{-} - N_{+2}) \left[- \frac{9533}{108}S_2 + 8S_{2,-3} - \frac{77}{3}S_{2,-2} - 8S_{2,-2,1} \right. \\ & - 8S_{2,1,-2} - \frac{44}{3}S_{2,2} - \frac{1517}{18}S_3 + 8S_{3,-2} - \frac{121}{3}S_{3,1} + 4S_{3,2} + 44S_4 + 16S_{4,1} - 8S_5 \left. \right] \\ & + (1 - N_{+}) \left[\frac{8533}{108}S_2 - 8S_{2,-3} + \frac{103}{3}S_{2,-2} + 8S_{2,-2,1} + \frac{109}{9}S_{2,1} + 8S_{2,1,-2} + \frac{28}{3}S_{2,2} \right. \\ & \left. + \frac{1579}{18}S_3 + 8S_{3,-2} + \frac{71}{3}S_{3,1} - 4S_{3,2} - \frac{98}{3}S_4 - 16S_{4,1} + 36S_5 \right] - \frac{79}{32} + 4S_{-5} - 8S_{-4,1} \end{aligned}$$

$$\begin{aligned}
& + \frac{67}{9}S_{-3} - 4S_{-3,-2} - 2S_{-3,2} - 4S_{-2,-3} - \frac{11}{3}S_{-2,-2} + 4S_{-2,-2,1} + 4S_{-2,1,-2} \\
& - \frac{16619}{162}S_1 - \frac{88}{3}S_{1,-3} - \frac{523}{18}S_{1,-2} + 11S_{1,-2,1} + \frac{413}{108}S_{1,1} - 11S_{1,1,-2} - \frac{67}{9}S_{1,2} \\
& - \frac{33}{2}S_{1,3} + \frac{781}{54}S_2 - 4S_{2,-3} + \frac{11}{3}S_{2,-2} + 4S_{2,-2,1} - \frac{67}{9}S_{2,1} + 4S_{2,1,-2} - \frac{22}{3}S_{2,2} \\
& + \frac{67}{9}S_3 - 4S_{3,-2} + \frac{11}{6}S_{3,1} - 2S_{3,2} - 8S_{4,1} + 4S_5 \Big) . \tag{3.3}
\end{aligned}$$

Note that harmonic sums up to weight $2n + 1$ occur at order α_s^{n+1} (N^n LO).

We stress that Eqs. (3.2) and (3.3) are directly applicable only for even positive values of N , while the lowest-order expression (3.1) holds for any positive integer. For general (non-integer) N , $\gamma^{(n)}(N)$ can be obtained by numerically evaluating

$$\gamma^{(n)}(N) = - \int_0^1 dx x^{N-1} P^{(n)}(x) \tag{3.4}$$

using the x -space results to which we turn now.

3.2 Expressions in Bjorken- x space

There is a theorem [31] ensuring that the splitting functions $P^{(n)}(x)$ can be uniquely reconstructed from their even- N (or odd- N) moments obtained in our calculations. In fact, the close relation between the harmonic sums and the harmonic polylogarithms facilitates an algebraic procedure [38,39] for the inverse Mellin transform.

For a compact representation of the gluon-gluon splitting functions we use

$$p_{gg}(x) \equiv (1-x)^{-1} + x^{-1} - 2 + x - x^2$$

and an abbreviation for the harmonic polylogarithms [38],

$$H_{\pm(m+1), \pm(n+1), \dots} \equiv H_{\underbrace{0, \dots, 0}_m, \underbrace{\pm 1, 0, \dots, 0}_n, \pm 1, \dots}(x) .$$

The one- and two-loop results [5,9] for $n_f = 0$ can then be written as

$$P_{gg}^{(0)}(x) = C_A \left(4p_{gg}(x) + \frac{11}{3} \delta(1-x) \right) , \tag{3.5}$$

$$\begin{aligned}
P_{gg}^{(1)}(x) = & 4C_A^2 \left(2p_{gg}(x) \left[\frac{67}{18} - \zeta_2 + H_{0,0} + 2H_{1,0} + 2H_2 \right] - 2p_{gg}(-x) \left[\zeta_2 + 2H_{-1,0} \right. \right. \\
& \left. \left. - H_{0,0} \right] - \frac{67}{9} \left(\frac{1}{x} - x^2 \right) - \frac{44}{3} x^2 H_0 + (1+x) \left[\frac{11}{3} H_0 + 8H_{0,0} - \frac{27}{2} \right] + 27 - 12H_0 \right. \\
& \left. + \delta(1-x) \left[\frac{8}{3} + 3\zeta_3 \right] \right) . \tag{3.6}
\end{aligned}$$

The corresponding three-loop contribution [2] reads

$$\begin{aligned}
P_{gg}^{(2)}(x) = & 16C_A^3 \left(p_{gg}(x) \left[\frac{245}{24} - \frac{67}{9}\zeta_2 + \frac{11}{3}\zeta_3 - \frac{3}{10}\zeta_2^2 - 4H_{-3,0} + 6H_{-2}\zeta_2 + 4H_{-2,-1,0} \right. \right. \\
& + \frac{11}{3}H_{-2,0} - 4H_{-2,0,0} - 4H_{-2,2} + \frac{1}{6}H_0 - 7H_0\zeta_3 + \frac{67}{9}H_{0,0} - 8H_{0,0}\zeta_2 + 4H_{0,0,0,0} - 6H_1\zeta_3 \\
& \left. \left. - 4H_{1,-2,0} + \frac{134}{9}H_{1,0} - 6H_{1,0}\zeta_2 + \frac{11}{6}H_{1,0,0} + 8H_{1,0,0,0} + 8H_{1,1,0,0} + 8H_{1,2,0} + 8H_{1,3} \right] \right) .
\end{aligned}$$

$$\begin{aligned}
& + \frac{134}{9} H_2 - 4 H_2 \zeta_2 + 10 H_{2,0,0} + 8 H_{2,1,0} + 8 H_{2,2} + \frac{11}{6} H_3 + 10 H_{3,0} + 8 H_{3,1} + 8 H_4 \Big] \\
& + p_{gg}(-x) \Big[-\frac{67}{9} \zeta_2 + \frac{11}{2} \zeta_2^2 - 4 H_{-3,0} + 16 H_{-2} \zeta_2 + 8 H_{-2,-1,0} - 18 H_{-2,0,0} - 12 H_{-2,2} \\
& + 12 H_{-1} \zeta_3 + 8 H_{-1,-2,0} - 16 H_{-1,-1} \zeta_2 + 24 H_{-1,-1,0,0} + 16 H_{-1,-1,2} - \frac{134}{9} H_{-1,0} \\
& + 18 H_{-1,0} \zeta_2 - 16 H_{-1,0,0,0} - 4 H_{-1,2,0} - 16 H_{-1,3} - \frac{11}{6} H_0 \zeta_2 - 5 H_0 \zeta_3 + \frac{67}{9} H_{0,0} - 8 H_{0,0} \zeta_2 \\
& + 4 H_{0,0,0,0} + 2 H_2 \zeta_2 + 2 H_{3,0} + 8 H_4 \Big] + \left(\frac{1}{x} - x^2 \right) \Big[\frac{16619}{162} - \frac{55}{2} \zeta_3 - \frac{11}{2} H_0 \zeta_2 - \frac{413}{108} H_1 \\
& - \frac{11}{2} H_1 \zeta_2 - \frac{67}{9} H_{1,0} + \frac{33}{2} H_{1,0,0} - \frac{67}{9} H_2 + \frac{22}{3} H_{2,0} \Big] + 11 \left(\frac{1}{x} + x^2 \right) \Big[-\frac{389}{198} \zeta_2 - \frac{2}{3} H_{-2,0} \\
& - \frac{1}{2} H_{-1} \zeta_2 + H_{-1,-1,0} - \frac{523}{198} H_{-1,0} + \frac{8}{3} H_{-1,0,0} + H_{-1,2} + \frac{71}{54} H_0 - \frac{1}{6} H_3 \Big] + x^2 \Big[\frac{85}{6} \zeta_2 \\
& + 33 H_{-2,0} + \frac{6409}{108} H_0 + 33 H_0 \zeta_2 - \frac{1249}{18} H_{0,0} - 44 H_{0,0,0} - \frac{44}{3} H_{2,0} - \frac{110}{3} H_3 \Big] \\
& + (1-x) \Big[-\frac{11317}{108} - 4 H_{-3,0} - 4 H_{-2} \zeta_2 - 8 H_{-2,-1,0} - \frac{19}{3} H_{-2,0} - 12 H_{-2,0,0} - \frac{263}{12} H_{0,0} \\
& - \frac{29}{3} H_{0,0,0} + \frac{31}{36} H_1 - \frac{3}{2} H_1 \zeta_2 + \frac{27}{2} H_{1,0} - \frac{25}{2} H_{1,0,0} \Big] + (1+x) \Big[-\frac{329}{18} \zeta_2 + \frac{11}{2} (1+x) \zeta_3 \\
& - \frac{43}{5} \zeta_2^2 - \frac{53}{2} H_{-1} \zeta_2 - 3 H_{-1,-1,0} - \frac{215}{6} H_{-1,0} + 38 H_{-1,0,0} + 25 H_{-1,2} + \frac{4651}{216} H_0 - 8 H_0 \zeta_3 \\
& + \frac{27}{2} H_0 \zeta_2 - 22 H_{0,0} \zeta_2 - \frac{158}{9} H_2 - 4 H_2 \zeta_2 + \frac{29}{3} H_{2,0} + 10 H_{2,0,0} - \frac{43}{6} H_3 + 16 H_{3,0} + 26 H_4 \Big] \\
& + \frac{53}{6} \zeta_2 + 24 \zeta_3 + 2 \zeta_2^2 - 16 H_{-3,0} + 27 H_{-2,0} + \frac{601}{12} H_0 + \frac{41}{3} H_0 \zeta_2 - 16 H_0 \zeta_3 - 29 H_{0,0} \\
& - 4 H_{0,0} \zeta_2 - \frac{40}{3} H_{0,0,0} + 28 x H_{0,0,0,0} + 27 H_2 - 24 H_{2,0} - 20 H_3 + \delta(1-x) \Big[\frac{79}{32} + \frac{1}{6} \zeta_2 \\
& + \frac{67}{6} \zeta_3 + \frac{11}{24} \zeta_2^2 - 5 \zeta_5 - \zeta_2 \zeta_3 \Big] \Big] , \tag{3.7}
\end{aligned}$$

where, as in Eqs. (3.5) and (3.6), all divergences for $x \rightarrow 1$ are to be read as $+$ -distributions. Functions $H_{\vec{m}}(x)$ up to weight (number of indices) $2n$ occur at N^n LO.

A FORTRAN program for the harmonic polylogarithms up to weight four is available [40]. Nevertheless it is useful to have also more compact, if approximate representations of the three-loop splitting functions. Making use of the end-point behaviour discussed in the next section, Eq. (3.7) can be parametrized as [2]

$$\begin{aligned}
P_{gg}^{(2)}(x) \cong & + 2643.521 \mathcal{D}_0 + 4425.894 \delta(1-x) + 3589 L_1 - 20852 + 3968 x \\
& - 3363 x^2 + 4848 x^3 + L_0 L_1 (7305 + 8757 L_0) + 274.4 L_0 \\
& - 7471 L_0^2 + 72 L_0^3 - 144 L_0^4 + 14214 x^{-1} + 2675.8 x^{-1} L_0 \tag{3.8}
\end{aligned}$$

where

$$\mathcal{D}_0 \equiv 1/(1-x)_+, \quad L_1 \equiv \ln(1-x), \quad L_0 \equiv \ln x.$$

This parametrization deviates from the exact expression (3.7) by less than 0.1%, which should be perfectly sufficient for numerical applications. Note that the Mellin transform of Eq. (3.8) can be readily continued to complex values of N as required for the moment-space approach to the analysis of hard processes [41]–[43].

4 Results and surprises for $x \rightarrow 1$ and $x \rightarrow 0$

The end-point behaviour of the splitting functions is of particular interest. The leading contributions for $x \rightarrow 1$ are related to the cusp anomalous dimensions and are thus relevant beyond the context of parton distributions. The perturbative stability at very small x , where potentially large $\ln^k x$ corrections occur, represents a much discussed topic directly relevant to analyses of collider processes.

4.1 The large- x behaviour

Up to $N^{n=2}\text{LO}$, at least, the diagonal $\overline{\text{MS}}$ -scheme splitting functions are given by

$$P_{\text{aa},x \rightarrow 1}^{(n)}(x) = \frac{A_{n+1}^{\text{a}}}{(1-x)_+} + B_{n+1}^{\text{a}} \delta(1-x) + C_{n+1}^{\text{a}} \ln(1-x) + \mathcal{O}(1). \quad (4.1)$$

In fact, the simple $+$ -distribution $1/(1-x)_+$ constitutes the leading term to all orders — in contrast to, for example, the coefficient functions in DIS which include terms $[(1-x)^{-1} \ln^k(1-x)]_+$ — and its coefficients A_m^{a} form the perturbative expansion of the cusp anomalous dimensions of the respective Wilson lines [44]. For the quark case the known coefficients read, in our normalization,

$$\begin{aligned} A_1^{\text{q}} &= 4 C_F \\ A_2^{\text{q}} &= 8 C_F \left[\left(\frac{67}{18} - \zeta_2 \right) C_A - \frac{5}{9} n_f \right] \\ A_3^{\text{q}} &= 16 C_F C_A^2 \left[\frac{245}{24} - \frac{67}{9} \zeta_2 + \frac{11}{6} \zeta_3 + \frac{11}{5} \zeta_2^2 \right] + 16 C_F^2 n_f \left[-\frac{55}{24} + 2 \zeta_3 \right] \\ &\quad + 16 C_F C_A n_f \left[-\frac{209}{108} + \frac{10}{9} \zeta_2 - \frac{7}{3} \zeta_3 \right] + 16 C_F n_f^2 \left[-\frac{1}{27} \right]. \end{aligned} \quad (4.2)$$

The coefficients A_m^{g} are obtained from Eq. (4.2) by multiplication with C_A/C_F . Note that the n_f -independent parts of A_m^{a} consist of only one (the maximally non-abelian) colour factor as also predicted in ref. [44]. The $n_f=0$ part of A_3^{q} and the complete A_3^{g} are new results of refs. [1] and [2], respectively. Two computations of the n_f -contribution to A_3^{q} were performed two years ago [20,22], and its n_f^2 -part was already obtained in ref. [15]. A_3^{q} in Eq. (4.2) agrees with the previous numerical estimate [45] which has been widely used in soft-gluon resummation analyses.

It is also interesting that at three loops, as in the previous order, only a single logarithm occurs in Eq. (4.1). Furthermore it turns out that there is an unexpected relation between the corresponding coefficients C_{n+1}^{a} and the A_n^{a} , viz [1,2]

$$C_1^{\text{a}} = 0, \quad C_2^{\text{a}} = (A_1^{\text{a}})^2, \quad C_3^{\text{a}} = 2 A_1^{\text{a}} A_2^{\text{a}}. \quad (4.3)$$

The logarithmic structure of Eq. (4.1) and especially the relation (4.3) call for an explanation and, possibly, a higher-order generalization.

The large- x limit of the quark-gluon and gluon-quark splitting functions reads

$$P_{ab,x \rightarrow 1}^{(n)}(x) = \sum_{i=0}^{2n-1} D_{n,i}^{\text{ab}} \ln^{2n-i}(1-x) + \mathcal{O}(1). \quad (4.4)$$

See ref. [2] for the three-loop coefficients $D_{2,i}^{\text{ab}}$. Except for $D_{2,3}^{\text{gq}}$ these coefficients vanish for the choice $C_A = C_F = n_f$ leading to a $\mathcal{N} = 1$ supersymmetric theory.

4.2 The small- x behaviour

We start with the flavour non-singlet contributions which, in the present unpolarized case, are practically far less important than the singlet parts. However, the non-singlet small- x expansion includes two additional powers of $\ln x$ per order, i.e., terms up to $\ln^{2n} x$ occur at N^n LO. Thus the three-loop splitting functions

$$P_{x \rightarrow 0}^{(2)i=\pm,s}(x) = D_0^i \ln^4 x + \dots + D_3^i \ln x + \mathcal{O}(1) \quad (4.5)$$

form a presently unique theoretical laboratory for studying the relative size of as many as four small- x logarithms as obtained from a complete (all- x) calculation.

The numerical QCD values of the coefficients for $i = -$ in Eq. (4.5) read

$$\begin{aligned} D_0^- &\cong 1.4321 \\ D_1^- &\cong 35.556 - 3.1605 n_f \\ D_2^- &\cong 399.21 - 39.704 n_f + 0.5926 n_f^2 \\ D_3^- &\cong 1465.9 - 172.69 n_f + 4.3457 n_f^2 . \end{aligned} \quad (4.6)$$

See ref. [1] for the analytic expressions and the similar case $i = +$. In both cases the leading coefficients D_0 have been correctly predicted [18] on the basis of the resummation in ref. [46]. Note that the expansion (4.5) alternates for $i = \pm$, and that the coefficients D_k rise sharply with k . For $n_f = 4$ and $i = -$ shown in Fig. 2, the modulus of the $\ln^4 x$ ($\ln^3 x$) contribution is twice as large as that of the next term, $\ln^3 x$ ($\ln^2 x$), only at extremely small x -values, $x \lesssim 10^{-14}$ ($3 \cdot 10^{-10}$).

The numerical situation is rather different for the $d_{abc}d_{abc}$ contribution $i = s$ [1],

$$\begin{aligned} D_0^s &\cong +1.4815 n_f , \quad D_1^s \cong -2.9630 n_f \\ D_2^s &\cong +6.8918 n_f , \quad D_3^s \cong +178.03 n_f . \end{aligned} \quad (4.7)$$

Here the leading small- x terms do indeed provide a reasonable approximation, see Fig. 2. Note that the existence of a leading ($\ln^4 x$) $d_{abcd}d_{abc}$ contribution for $i = s$ is rather surprising. In fact, the presence of a leading small- x logarithm in a term unpredictable from lower-order structures appears to call into question the very concept of the small- x resummation of the double logarithms $\alpha_s^{n+1} \ln^{2n} x$.

The leading small- x terms of the three-loop singlet splitting functions are

$$P_{ab,x \rightarrow 0}^{(2)}(x) = E_1^{ab} \frac{\ln x}{x} + E_2^{ab} \frac{1}{x} + \mathcal{O}(\ln^4 x) . \quad (4.8)$$

In general, $x^{-1} \ln^k x$ contributions with $k \leq n$ occur in P_{gq} and P_{gg} at N^n LO. The highest of these terms ($k = n$) have, however, vanishing coefficients for $n = 1, 2$ as predicted by the leading-logarithmic BFKL equation [47,48], see also ref. [49].

In QCD the numerical values of the coefficients in Eq. (4.8) are given by

$$\begin{aligned} E_1^{qq} &\cong -132.74 n_f , \quad E_2^{qq} \cong -506.00 n_f + 3.1605 n_f^2 \\ E_1^{qg} &\cong -298.67 n_f , \quad E_2^{qg} \cong -1268.3 n_f + 4.5761 n_f^2 \\ E_1^{gq} &\cong 1189.3 + 71.083 n_f , \quad E_2^{gq} \cong 6163.1 - 46.408 n_f - 2.3704 n_f^2 \\ E_1^{gg} &\cong 2675.9 + 157.27 n_f , \quad E_2^{gg} \cong 14214. + 182.96 n_f - 2.7984 n_f^2 . \end{aligned} \quad (4.9)$$

The analytical results can be found in ref. [2]. The coefficients E_1^{qa} and E_1^{gg} agree with those derived from the small- x resummation in refs. [17] and [19], respectively, after transforming the latter result to the $\overline{\text{MS}}$ scheme [50]. E_1^{gq} was unknown before ref. [2]. For $n_f = 3 \dots 5$ the ratios $E_2^{\text{ab}}/E_1^{\text{ab}}$ are $3.7 \dots 4.7$. Thus the corrections due to the non-logarithmic $1/x$ terms amount to less than 50% only at $x \lesssim 10^{-4}$.

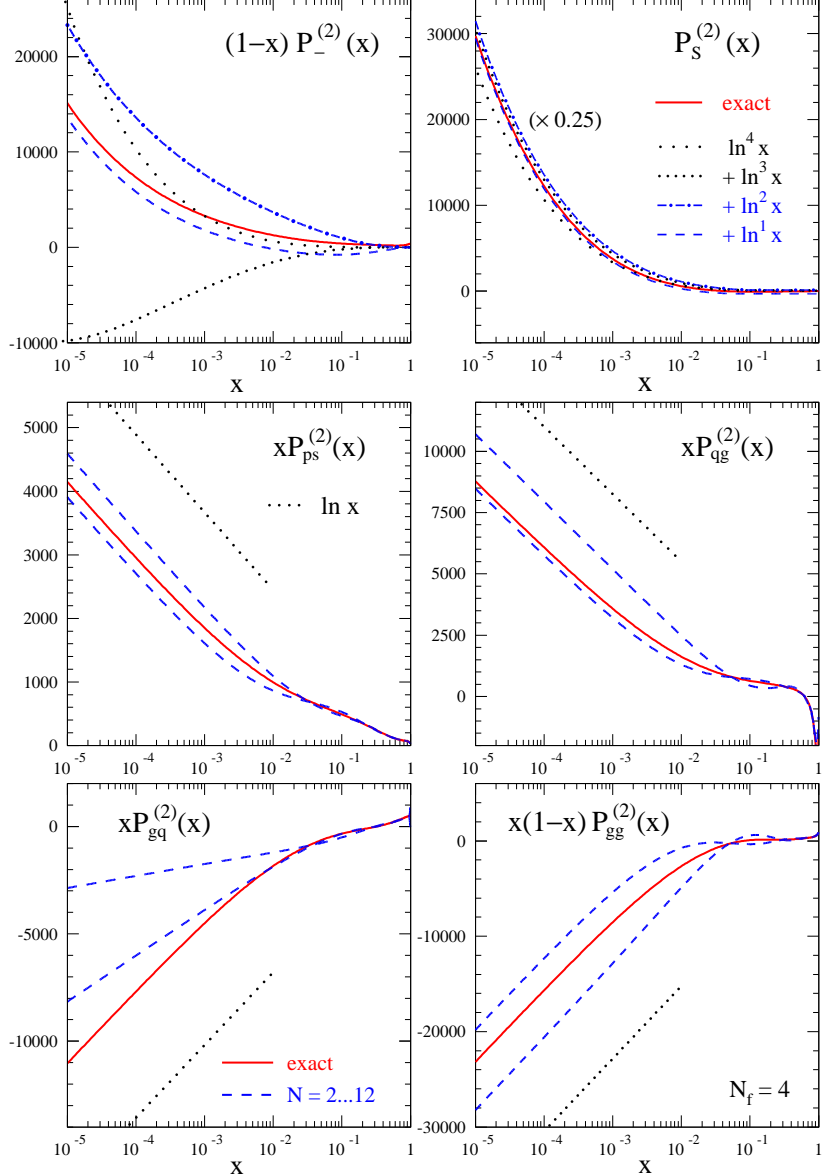


Figure 2. The small- x behaviour of non-singlet (upper row) and singlet NNLO splitting functions for $n_f = 4$. Also shown are the (successive) approximations (4.5) and (4.8) by the leading small- x logarithms and, for the singlet cases, the errors bands [51] used in the analyses of refs. [52,53].

5 The size of the corrections

Finally we discuss the numerical effects of our new contributions $P^{(2)}$ to Eq. (1.3). For brevity, we confine ourselves to four quark flavours and a typical scale $\mu^2 \simeq 30 \dots 50$ GeV². We employ an order-independent value of the strong coupling,

$$\alpha_s(\mu_0^2, n_f = 4) = 0.2 , \quad (5.1)$$

facilitating a direct comparison of the $\overline{\text{MS}}$ evolution kernels at LO, NLO and NNLO.

5.1 N -space: anomalous dimensions

The singlet anomalous dimensions $\gamma_{ff'}$ are displayed in Fig. 3 for the standard choice $\mu_r = \mu_f$ of the renormalization scale tacitly made already in sections 3 and 4. The NNLO corrections are markedly smaller than the NLO contributions. For the choice (5.1) they amount, at $N > 2$, to less than 2% and 1% for the large diagonal quantities γ_{qq} and γ_{gg} , respectively, while for the much smaller off-diagonal anomalous dimensions γ_{qg} and γ_{gq} values of up to 6% and 4% are reached. Also shown in Fig. 3 is the pure-singlet contribution γ_{ps} defined by Eq. (2.8). At $N > 2$ this quantity receives very large relative (but tiny absolute) NNLO corrections.

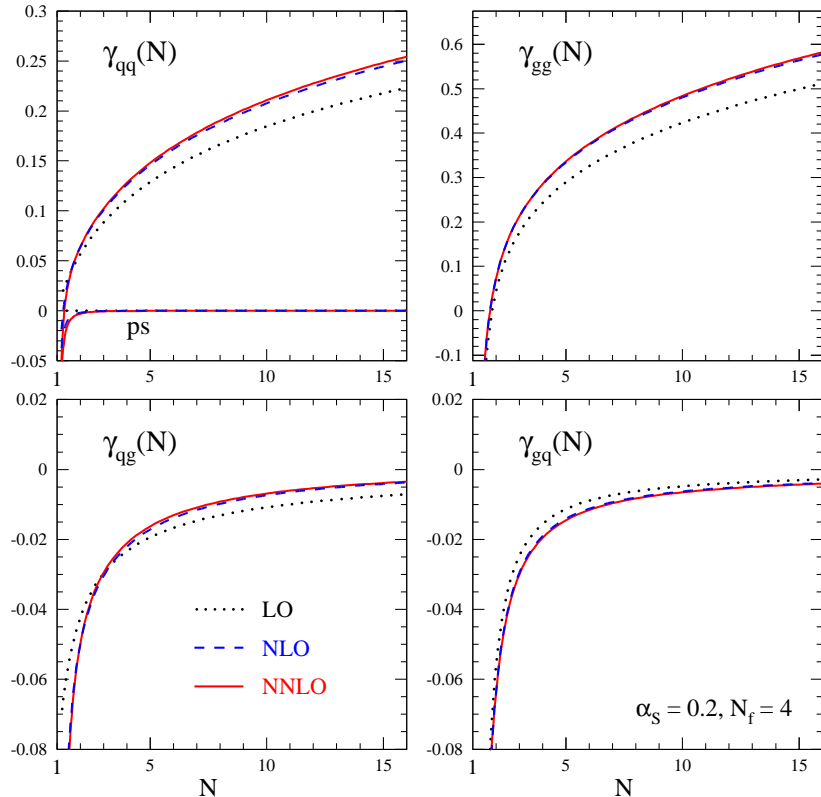


Figure 3. The perturbative expansion of the singlet anomalous dimensions $\gamma_{ff'}$ up to NNLO.

5.2 Scale derivatives of x -space parton distributions

In Figs. 4 and 5 we show the logarithmic derivatives $\dot{f}_k = d \ln f_k / d \ln \mu_f^2$ for the sufficiently realistic – and like Eq. (5.1) order-independent – model distributions

$$\begin{aligned} xq_{ns}(x, \mu_0^2) &= x^{0.5} (1-x)^3 \\ xq_s(x, \mu_0^2) &= 0.6 x^{-0.3} (1-x)^{3.5} (1 + 5.0 x^{0.8}) \\ xg(x, \mu_0^2) &= 1.6 x^{-0.3} (1-x)^{4.5} (1 - 0.6 x^{0.3}) . \end{aligned} \quad (5.2)$$

At large x the NNLO corrections to the non-singlet evolution illustrated in Fig. 4 are very similar for all three cases (2.5). They amount to 2% or less for $x \geq 0.2$, thus being smaller than the NLO contributions by a factor of about eight. For q_{ns}^- the same suppression is also found in the region $10^{-5} \lesssim x \lesssim 10^{-2}$. The NNLO effects are even smaller for q_{ns}^+ (not shown) at small x , but considerably larger for q_{ns}^v at $x < 10^{-3}$ due to the additional effect of the new quantity P_{ns}^s in Eq. (2.6).

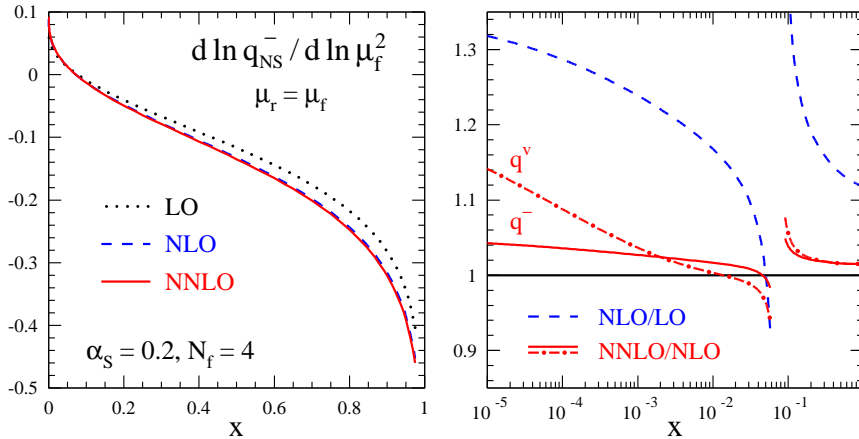


Figure 4. The perturbative expansion up to NNLO of the factorization-scale derivatives $\dot{q}_{ns}^{-,v}$ for the initial conditions (5.1), (5.2) and the standard choice $\mu_r = \mu_f$ of the renormalization scale.

Also for the singlet quark distribution (upper row of Fig. 5) the ratio of the NLO and NNLO corrections is about eight over the full x -range. However, at small x – where $P_{qg} * g$ dominates in Eq. (2.7) – the LO results are anomalously small as P_{qq} and P_{qg} , unlike at higher orders, do not include $1/x$ terms at first order. The situation is quite different for the evolution of the gluon density (dominated by $P_{gg} * g$ at all x). Here the NLO contributions appear atypically small at low x , cf. the remark below Eq. (4.8). Thus the ratio of the NNLO and NLO corrections is rather large here, despite the former amounting to only 3% for x as low as 10^{-4} .

It is also interesting to consider the stability of the above results under variations of the renormalization scale μ_r . For $\mu_r \neq \mu_f$ the perturbative expansion of the splitting functions up to NNLO reads, with $L_{fr} \equiv \ln(\mu_f^2/\mu_r^2)$,

$$\begin{aligned} P &= a_s(\mu_r^2) P^{(0)} + a_s^2(\mu_r^2) (P^{(1)} - \beta_0 P^{(0)} L_{fr}) \\ &+ a_s^3(\mu_r^2) (P^{(2)} - \{\beta_1 P^{(0)} + 2\beta_0 P^{(1)}\} L_{fr} + \beta_0^2 P^{(0)} L_{fr}^2) . \end{aligned} \quad (5.3)$$

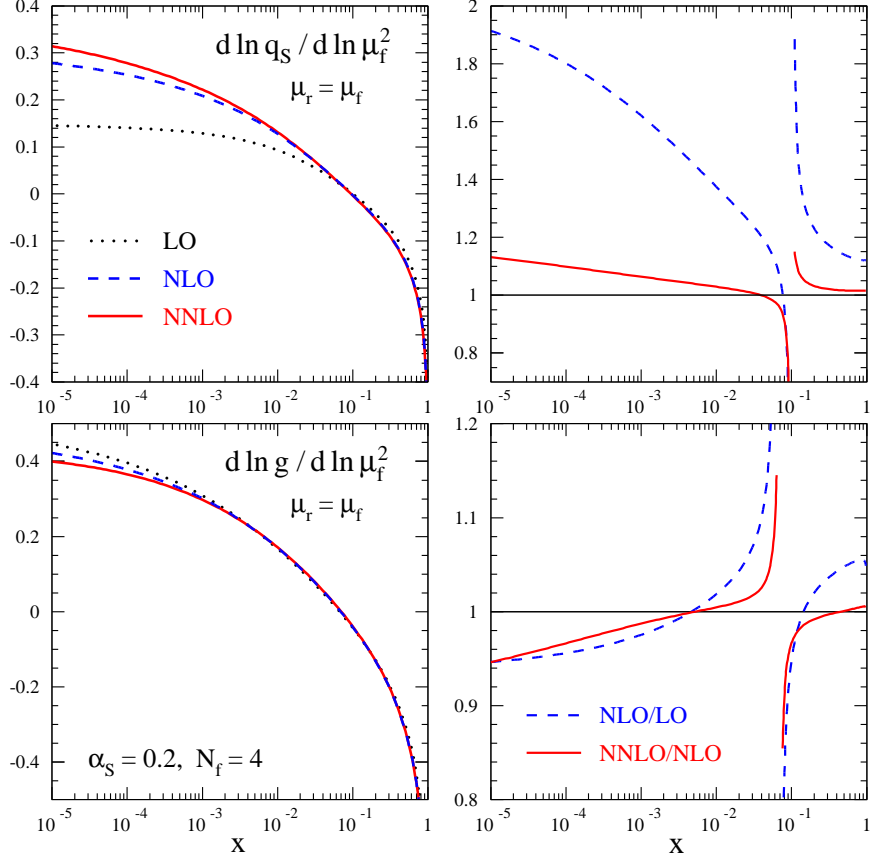


Figure 5. As Fig. 4, but for the singlet quark and gluon distributions q_s and g . The spikes close $x = 0.1$ in the right plots reflect the zeros of \dot{f}_k and do not constitute large absolute corrections.

Here $a_s(\mu_r^2)$ is obtained at $N^n\text{LO}$ from the value (5.1) at the scale μ_0^2 by solving

$$\frac{da_s}{d \ln \mu_r^2} = \beta(a_s) = - \sum_{l=0}^n a_s^{k+2} \beta_k . \quad (5.4)$$

The $\overline{\text{MS}}$ expansion coefficients β_k are presently known up to $k = 3$ [54]–[58].

The dependence of the above results on μ_r can be found in Fig. 8 of ref. [1] and Figs. 9 and 10 of ref. [2] for selected values of x . Here we only show, in Fig. 6, the relative scale uncertainties $\Delta \dot{f}_k$ of the average μ_f -derivatives as conventionally estimated by varying μ_r up to a factor of two with respect to μ_f ,

$$\Delta \dot{f} = \frac{\max \dot{f} - \min \dot{f}}{2 |\text{average } \dot{f}|} , \quad \mu_r^2 = \frac{1}{4} \mu_f^2 \dots 4 \mu_f^2 . \quad (5.5)$$

For the valence, (singlet-quark, gluon) distributions, these uncertainty estimates amount to 3% (3%, 1%) or less at $x > 5 \cdot 10^{-4}$ ($5 \cdot 10^{-3}$, $3 \cdot 10^{-4}$), an improvement by more than a factor of three with respect to the corresponding NLO results.

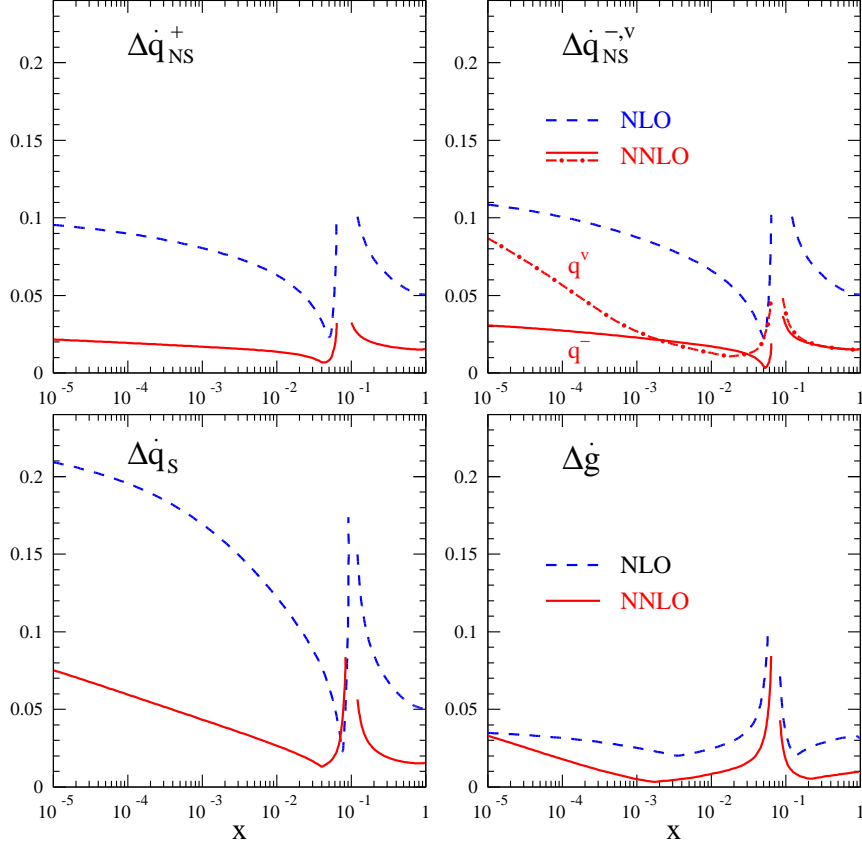


Figure 6. The renormalization scale uncertainties of the NLO and NNLO predictions for the evolution of the non-singlet and singlet distributions as estimated by the quantities $\Delta\dot{f}_k$ in Eq. (5.5).

6 Summary and outlook

We have calculated the complete third-order splitting functions for the evolution of unpolarized parton distributions in perturbative QCD. The computation is performed in Mellin- N space and follows the previous fixed- N computations [12]–[14] inasmuch as we compute the partonic structure functions in deep-inelastic scattering at even or odd N . Our calculation, however, provides the complete N -dependence from which the splitting functions in Bjorken- x space can be uniquely reconstructed.

A salient feature of our approach is that it facilitates very efficient checks of our elaborate schemes for the reduction of the required three-loop integrals by using the MINCER program [24,25]. By keeping terms of order ε^0 in dimensional regularization throughout the calculation, we have also obtained the third-order coefficient functions for the structure functions F_2 and F_L in electromagnetic and for F_3 in charged-current DIS [23]. The present method can be used to generalize our fixed- N three-loop calculation of the photon structure [59] to all N . It should also be possible to obtain the polarized NNLO splitting function in this manner.

Our results completely agree with all partial results available in the literature for fixed moments [12]–[14], large- n_f limits [15,16], small- x behaviour [17]–[19] and large- x structure [22,44]. With the (relatively unimportant) exception of P_{gq} shown above and P_{ns}^s they also fully agree with the uncertainty bands of ref. [51] used in provisional NNLO analyses [52,53]. Those analyses thus remain valid. The results do, however, exhibit some unexpected features, most notably a suggestive relation between large- x coefficients and the presence of a leading small- x term in the new $d_{abc}d_{abc}$ contribution P_{ns}^s to the splitting function for the valence distribution.

The effect of the three-loop (NNLO) corrections on the evolution of the parton densities is small at $x \gtrsim 10^{-3}$. For $\alpha_s = 0.2$, for example, both the corrections and the μ_r variation amount to less than 2% at large x ; and the NNLO effects are about eight times smaller than the NLO contributions, implying that the evolution is perturbatively stable down to rather low scales. For $x < 10^{-3}$ the corrections increase with decreasing x . As the knowledge of the leading small- x terms is not sufficient, further improvements in this region would require considerable efforts, including at least an extension of the MINCER program [24,25] to four loops.

References

1. S. Moch, J.A.M. Vermaseren and A. Vogt, Nucl. Phys. B688 (2004) 101, hep-ph/0403192
2. A. Vogt, S. Moch and J.A.M. Vermaseren, Nucl. Phys. B691 (2004) 129, hep-ph/0404111
3. D.J. Gross and F. Wilczek, Phys. Rev. D8 (1973) 3633
4. H. Georgi and H.D. Politzer, Phys. Rev. D9 (1974) 416
5. G. Altarelli and G. Parisi, Nucl. Phys. B126 (1977) 298
6. E.G. Floratos, D.A. Ross and C.T. Sachrajda, Nucl. Phys. B129 (1977) 66
7. E.G. Floratos, D.A. Ross and C.T. Sachrajda, Nucl. Phys. B152 (1979) 493
8. G. Curci, W. Furmanski and R. Petronzio, Nucl. Phys. B175 (1980) 27
9. W. Furmanski and R. Petronzio, Phys. Lett. 97B (1980) 437
10. E.G. Floratos, C. Kounnas and R. Lacaze, Nucl. Phys. B192 (1981) 417
11. R. Hamberg and W.L. van Neerven, Nucl. Phys. B379 (1992) 143
12. S. Larin, T. van Ritbergen, and J. Vermaseren, Nucl. Phys. B427 (1994) 40
13. S. Larin, P. Nogueira, T. van Ritbergen and J. Vermaseren, Nucl. Phys. B492 (1997) 338, hep-ph/9605317
14. A. Retey and J. Vermaseren, Nucl. Phys. B604 (2001) 281, hep-ph/0007294
15. J.A. Gracey, Phys. Lett. B322 (1994) 141, hep-ph/9401214
16. J.F. Bennett and J.A. Gracey, Nucl. Phys. B517 (1998) 241, hep-ph/9710364
17. S. Catani and F. Hautmann, Nucl. Phys. B427 (1994) 475, hep-ph/9405388
18. J. Blümlein and A. Vogt, Phys. Lett. B370 (1996) 149, hep-ph/9510410
19. V.S. Fadin and L.N. Lipatov, Phys. Lett. B429 (1998) 127, hep-ph/9802290
20. S. Moch, J.A.M. Vermaseren and A. Vogt, Nucl. Phys. B646 (2002) 181, hep-ph/0209100
21. J. Vermaseren, S. Moch and A. Vogt, Nucl. Phys. Proc. Suppl. 116 (2003) 100, hep-ph/0211296
22. C.F. Berger, Phys. Rev. D66 (2002) 116002, hep-ph/0209107

23. J.A.M. Vermaseren, A. Vogt and S. Moch, in preparation
24. S.G. Gorishnii et al., Comput. Phys. Commun. 55 (1989) 381
25. S.A. Larin, F.V. Tkachev and J.A.M. Vermaseren, NIKHEF-H-91-18
26. S. Larin and J. Vermaseren, Phys. Lett. B259 (1991) 345
27. W.L. van Neerven and E.B. Zijlstra, Phys. Lett. B272 (1991) 127
28. E.B. Zijlstra and W.L. van Neerven, Phys. Lett. B273 (1991) 476
29. E.B. Zijlstra and W.L. van Neerven, Phys. Lett. B297 (1992) 377
30. E.B. Zijlstra and W.L. van Neerven, Nucl. Phys. B383 (1992) 525
31. F.J. Ynduráin, *The Theory of Quark and Gluon Interactions*, 3rd edition, (Springer 1999) and references therein.
32. H. Kluberg-Stern and J.B. Zuber, Phys. Rev. D12 (1975) 467
33. J.C. Collins, A. Duncan, and S.D. Joglekar, Phys. Rev. D16 (1977) 438
34. P. Nogueira, J. Comput. Phys. 105 (1993) 279
35. J.A.M. Vermaseren, math-ph/0010025
36. J.A.M. Vermaseren, Nucl. Phys. Proc. Suppl. 116 (2003) 343, hep-ph/0211297
37. J.A.M. Vermaseren, Int. J. Mod. Phys. A14 (1999) 2037, hep-ph/9806280
38. E. Remiddi and J.A.M. Vermaseren, Int. J. Mod. Phys. A15 (2000) 725, hep-ph/9905237
39. S. Moch and J. Vermaseren, Nucl. Phys. B573 (2000) 853, hep-ph/9912355
40. T. Gehrmann and E. Remiddi, Comput. Phys. Commun. 141 (2001) 296, hep-ph/0107173
41. Ch. Berger, D. Graudenz, M. Hampel and A. Vogt, Z. Phys. C70 (1996) 77, hep-ph/9506333
42. D. A. Kosower, Nucl. Phys. B520 (1998) 263, hep-ph/9708392
43. M. Stratmann and W. Vogelsang, Phys. Rev. D64 (2001) 114007, hep-ph/0107064
44. G. P. Korchemsky, Mod. Phys. Lett. A4 (1989) 1257
45. A. Vogt, Phys. Lett. B497 (2001) 228, hep-ph/0010146
46. R. Kirschner and L.N. Lipatov, Nucl. Phys. B213 (1983) 122
47. E.A. Kuraev, L.N. Lipatov and V.S. Fadin, Sov. Phys. JETP 45 (1977) 199
48. I.I. Balitsky and L.N. Lipatov, Sov. J. Nucl. Phys. 28 (1978) 822
49. T. Jaroszewicz, Phys. Lett. B116 (1982) 291.
50. W.L. van Neerven and A. Vogt, Nucl. Phys. B588 (2000) 345, hep-ph/0006154
51. W.L. van Neerven and A. Vogt, Phys. Lett. B490 (2000) 111, hep-ph/0007362
52. A.D. Martin, R.G. Roberts, W.J. Stirling and R.S. Thorne, Phys. Lett. B531 (2002) 216, hep-ph/0201127
53. S. Alekhin, Phys. Rev. D68 (2003) 014002, hep-ph/0211096
54. W.E. Caswell, Phys. Rev. Lett. 33 (1974) 244
55. D.R.T. Jones, Nucl. Phys. B75 (1974) 531
56. O.V. Tarasov, A.A. Vladimirov, and A.Y. Zharkov, Phys. Lett. 93B (1980) 429
57. S. Larin and J. Vermaseren, Phys. Lett. B303 (1993) 334, hep-ph/9302208
58. T. van Ritbergen, J. Vermaseren and S. Larin, Phys. Lett. B400 (1997) 379, hep-ph/9701390
59. S. Moch, J.A.M. Vermaseren and A. Vogt, Nucl. Phys. B621 (2002) 413, hep-ph/0110331